

Multi-Decadal Seawall-Induced Topo-Bathymetric Perturbations along a Highly Energetic Coast

Alexandre Nicolae Lerma, Julie Billy, Thomas Bulteau, Cyril Mallet

▶ **To cite this version:**

Alexandre Nicolae Lerma, Julie Billy, Thomas Bulteau, Cyril Mallet. Multi-Decadal Seawall-Induced Topo-Bathymetric Perturbations along a Highly Energetic Coast. Journal of Marine Science and Engineering, 2022, 10 (4), pp.503. 10.3390/jmse10040503 . hal-03659813

HAL Id: hal-03659813
https://brgm.hal.science/hal-03659813

Submitted on 5 May 2022

HAL is a multi-disciplinary open access archive for the deposit and dissemination of scientific research documents, whether they are published or not. The documents may come from teaching and research institutions in France or abroad, or from public or private research centers.

L'archive ouverte pluridisciplinaire **HAL**, est destinée au dépôt et à la diffusion de documents scientifiques de niveau recherche, publiés ou non, émanant des établissements d'enseignement et de recherche français ou étrangers, des laboratoires publics ou privés.



Distributed under a Creative Commons Attribution 4.0 International License

Journal of *Marine Science and Engineering*

MDPI

Article

Multi-Decadal Seawall-Induced Topo-Bathymetric Perturbations along a Highly Energetic Coast

Alexandre Nicolae Lerma [1,2,*], Julie Billy [1], Thomas Bulteau [1,2] and Cyril Mallet [1,2]

[1] Brgm Regional Direction Nouvelle-Aquitaine, 33600 Pessac, France; j.billy@brgm.fr (J.B.); t.bulteau@brgm.fr (T.B.); c.mallet@brgm.fr (C.M.)
[2] OCNA Observatoire de la Côte de Nouvelle-Aquitaine, 33600 Pessac, France
* Correspondence: a.nicolaelerma@brgm.fr

Abstract: Seawalls are commonly used worldwide to protect urbanized sea fronts. These alongshore protection structures are often blamed for hydro-sedimentary dynamics perturbations, but without clear and generalizable conclusions on long-term morphodynamic effects. In this paper, evolutions of beaches are studied from 1966 to 2021, comparing the urbanized sea front of Lacanau seaside resort (Aquitaine France) and adjacent natural areas. A large-scale spatiotemporal multisource dataset is used to derivate several indicators and evaluate the characteristics and magnitude of passive and active erosion related to a large riprap seawall at a highly energetic meso–macro tidal coast. The most dramatic manifestation of the presence of the seawall (passive erosion) is the beach lowering and the reduction of beach variability at the seasonal and interannual timescale in front of the seawall. However, recent evolutions are roughly similar at the seawall-backed beach than at the natural sector, indicating no specific active seawall influence on beach erosion or recovery. The perturbations directly attributable to the seawall (active erosion) are limited to temporary end-effect, slight perturbation of outer bar pattern and the setup of a slight platform around the depth of closure. The adverse effects are currently manageable, but they require a new strategy in view of the chronic shoreline retreat at adjacent sectors and the expected effects of climate change.

Keywords: coastal erosion; coastal structure; beach recovery; LiDAR; aquitaine coast

check for updates

Citation: Lerma, A.N.; Billy, J.; Bulteau, T.; Mallet, C. Multi-Decadal Seawall-Induced Topo-Bathymetric Perturbations along a Highly Energetic Coast. *J. Mar. Sci. Eng.* **2022**, *10*, 503. https://doi.org/10.3390/jmse10040503

Academic Editor: Enzo Pranzini

Received: 26 February 2022
Accepted: 30 March 2022
Published: 6 April 2022

Publisher's Note: MDPI stays neutral with regard to jurisdictional claims in published maps and institutional affiliations.

Copyright: © 2022 by the authors. Licensee MDPI, Basel, Switzerland. This article is an open access article distributed under the terms and conditions of the Creative Commons Attribution (CC BY) license (https://creativecommons.org/licenses/by/4.0/).

1. Introduction

Along worldwide coasts, seaside resorts are commonly bordered by hard protections. Among existing solutions, seawalls are used in order to directly preserve urban areas from storm impacts and chronical erosion (see References [1,2] for examples). Seawalls are recognized to be efficient shore-protection structures to preserve local assets. However, on sandy coasts, they are commonly blamed for the perturbations of the hydro-sedimentary dynamics and beach morphology [3]. Beach lowering or disappearance of walled-backed beaches is, for example, a usual observation [4].

Perturbations related to seawalls depend upon several factors, such as the sedimentary context and shoreline evolution [5,6], the type and design of the structure [7,8], wave conditions [3,9–11], the characteristics of the beach water table [12] or the position of the seawall relative to the shoreline [4]. This last point is crucial to evaluate the impact of the seawall on the topo-bathymetric beach profiles [13–15]. Other authors have reported contrasting conclusions about adverse effect, such as scours at the base of the wall [16–19] or end-effect, at the directly adjacent shore [6,20–22]. Despite many studies performed since the 1980s, no definitive consensus on the mechanism and the magnitude of this perturbation was clearly reached [19,22,23], and questions about the active contribution of seawalls to erosion on beaches are still matters of debate [2].

In fact, due to the difficulties in capturing details of the hydro-sedimentary processes occurring on the field, physical modeling or laboratory studies have been preferred, and

the expected beach evolution, as well as bathymetric evolution near the seawalls, remains mostly theoretical [14–24]. Analyzing beach profiles of a beach backed by seawall on beach profile relatively to an adjacent unwalled beach is a classic approach to characterize the seawall impact on field studies [12,25–27]. However, most of them are restricted to simple topographic proxies [5,6] or to analyzing the seawall impact on the beach after storms [11,28,29]. Long-term surveys (decades and longer) are scarcer and rarely exceed a few years [30,31]. Furthermore, they mostly focus on beach topography along few beach profiles, without considering bathymetric data.

In this paper, we study the topo-bathymetric evolutions of the Lacanau seaside resort located at the meso–macro tidal, highly energetic Atlantic French coast. In this context, and in the long term (more than a decade), we investigated if specific geomorphological responses of the nearshore–beach–dune system are attributable to the presence of a large riprap seawall. According to the best of authors' knowledge, no previous study has compiled such multisource large-scale variable spatial and temporal coverage data (i.e., Orthophoto, DGPS, topographic airborne LiDAR and Echo-sounder bathymetry) in order to provide complete multi-proxy analysis of long-term seawall induced perturbation. Evolutions of beaches of the sea front of Lacanau were analyzed over the period 1966–2020 based on several indicators, including shoreline position, topo-bathymetric contours, beach morphology and sediment volume. The characteristics and magnitude of the perturbations were evaluated and bring a comprehensive lecture of passive and active erosion. The period analyzed includes the outstandingly energetic 2013/2014 winter and subsequent periods that also provide insight into beach reconstruction in front of a large riprap seawall in comparison to adjacent sectors.

2. Site

The study site is located along the sandy coast of Aquitaine, in Gironde, France (Figure 1a). More precisely, it covers 15 km of straight coast around the iconic seaside resort of Lacanau Ocean.

2.1. Beach and Dunes

Beaches along this part of the coast are double-barred [32]. The inner intertidal bar shows most of the time a transverse bar and a rip morphology. In contrast, the outer subtidal bar is modally crescentic. In the sector of Lacanau, the mean alongshore averaged wavelength of the inner system is about 400 m [32], and the outer bar horns are generally around 800 to 1000 km spaced.

These sandbars are important for beach morphology and response to storms, as the nearshore sandbar morphologies are sometimes mirrored after storm events at the beach-dune system as megacusp embayments with cross-shore amplitude of an order of 1–10 m [33]. In brief, accretive megacusps on the upper beach are enforced by inner-bar rip channels with a spacing of around 100 m and a typical lifetime of a few months. In contrast, erosive megacusps cutting the dune form during severe-storm-driven erosive events, which are primarily enforced by the outer-bar morphology with a spacing of around 1000 m [34].

The subaerial beach–dune profile typically exhibits a berm after period of fair weather conditions, sometimes with superimposed beach cusps. The beach–dune interface shows incipient foredune and foredune scarps alternating in both time [35] and space [36]. The coastal dune system corresponds to a continuous dune fixed by vegetation, intimately connected to the sandy beaches. Considered as a "natural" ecosystem, these dunes have been, in general, maintained and managed by the National Forest Office (ONF) since the mid-19 century [37].

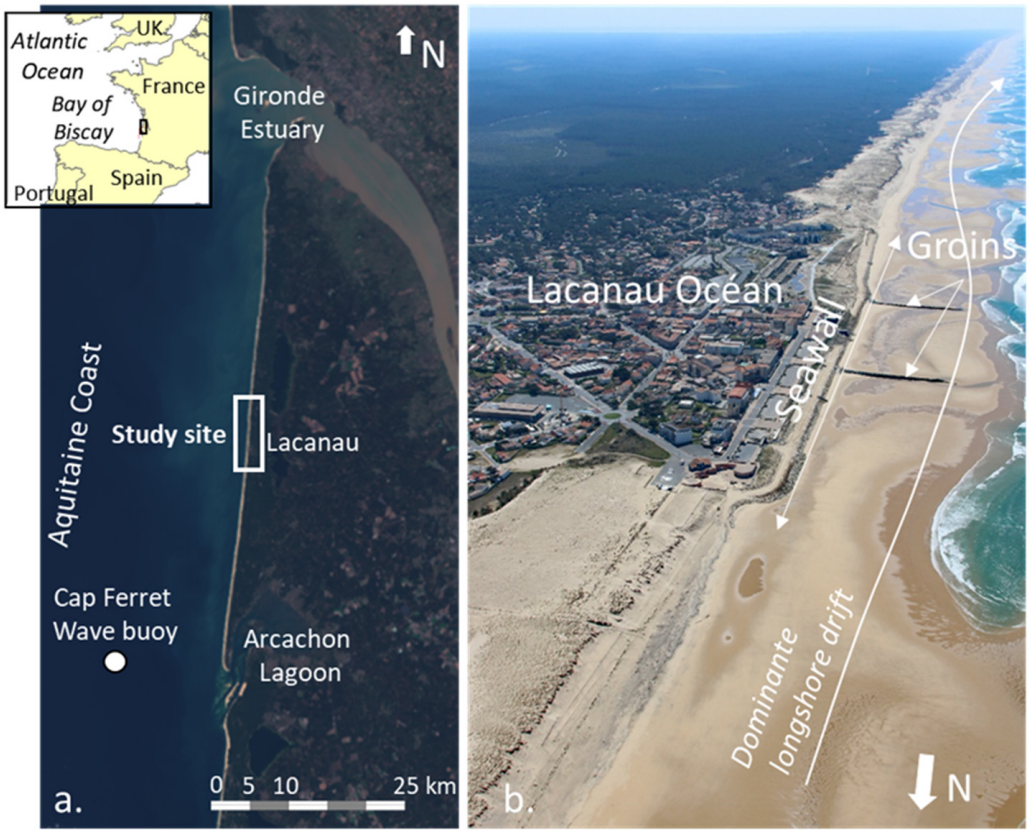


Figure 1. (**a**) Location of the study site at the center of the Gironde coast, SW France. (**b**) Aerial photograph of the sea front of Lacanau Ocean from the north, 10/04/2020 (photograph from the OCA database: OCA, taken by ULM Sud Bassin).

2.2. Long-Term Shoreline Evolution

The Gironde coast is in chronic state of erosion, exhibiting a large north–south gradient [38]. In the sector of Lacanau, several studies have evaluated the shoreline retreat during different period, supported by several kinds of information and proxies. Based on historic charts, the evolution rate has been evaluated to be between 0.3 and 0.5 m/year during the last century, period 1875–1967 [39]. Reference [40], which recounts a study based on ortho-photography interpretation, showed a general retreat in the sector but with significant longshore variability from 20 to 60 m between 1966 and 1998 (0.5 to 1.5 m/year). Shoreline change rates computed from a diachronic analysis of aerial photographs over the periods 1985–2014 [41] and 1950–2014 [42] show similar values of shoreline retreat (dune foot), which is, on average, around 2 m/year, but with a significant longshore variability between 0.5 and 3 m/year along a few kilometers. Since the outstanding 2013/2014 winter [43], which eroded the dune along almost the entire regional coast, no significant shoreline retreat has been observed in the area. The beach–dune at the adjacent beach of Lacanau has been slowly recovering and currently shows incipient foredunes at different stages of maturity [36].

2.3. Marine Forcings

The tide regime and wave climate are relatively homogeneous along the Nouvelle–Aquitaine coast. It is a mesotidal-to-macrotidal environment, with an annual mean tidal range of c. 3.7 m and a maximum tidal range reaching 5 m during spring tides, with a slightly lower tide range in the south. On the open coast, storm surge (non-tidal residual) is small (<1 m) [36].

The wave climate (Cap Ferret Buoys data) is energetic and strongly seasonally modulated with a monthly averaged significant wave height Hs (peak wave period Tp) that

ranges from 1.1 m (8.5 s) in July, with a dominant west–northwest direction, to 2.4 m (13 s) in January, with a dominant west direction [34]. The modal wave direction is from the west–northwest generating a southward oriented littoral drift, leading hereafter to consider the north of Lacanau, which is "upstream", and the south, which is "downstream".

Extreme wave conditions (the 100-year return Hs) are about 11.5 m [44]. Figure 2 shows the 2000–2020 time series of the wave energy flux, P (kW/m), calculated in deep water, according to the following equation [45]:

$$P = \frac{\rho g^2}{64\pi} T_p H_s^2 \quad (1)$$

where ρ is the density of sea water (1030 kg/m^3), and g the gravitational acceleration (9.81 m/s^2), with Hs and Tp extracted at the Cap Ferret buoy (in c. 50 m depth at 1.447° W and 44.653° N; see Figure 1a).

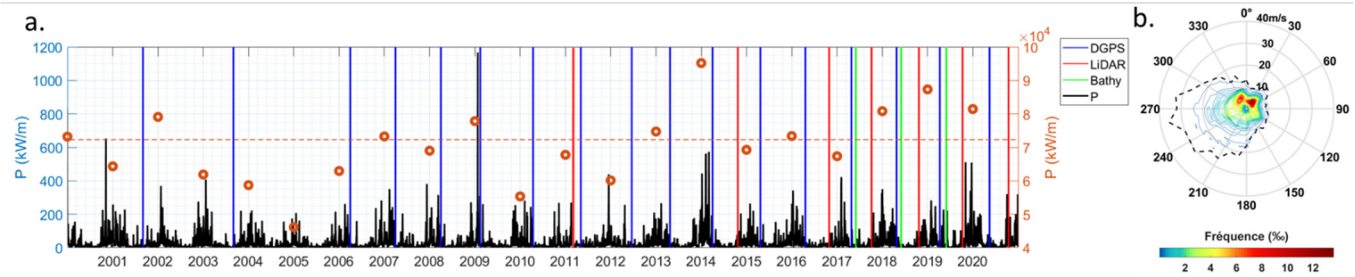


Figure 2. (**a**) Time series of computed wave energy flux (P) at Cap Ferret buoy location (Figure 1) over the period 2000–2020 (grid point hourly data). Vertical lines indicate the occurrence of topographic surveys by GNSS (blue), airborne topographic LiDAR (red) and bathymetric echo-sounding (green). Orange circle indicates the annual cumulated energy (right axis), and the dashed line is the mean annual cumulated energy calculated over the period. (**b**) Wind rose the Cap Ferret wind station (observations) for the same period.

In Figure 2, we can observe that the wave energy flux can have high interannual variability. After 2014, the last three years of the study period were the most energetic of the 20 last years.

2.4. Seafront Management

The site was progressively urbanized during the second half of the 20th century by extending the old town of Lacanau toward the coast. First the urbanization located at the back of the dune progressively developed over the first line dune by building villas, hotels and parking lots to facilitate beach access.

During the 1970s, to respond to the threat of erosion on the first building lines, the municipality decided to fix the coastline by using a longitudinal protection installed at the dune toe. The protection originally made of sheet pilling was rapidly supported by riprap blocs along 130 m [46]. Strong storms in 1979 damaged this seawall, which was rapidly fixed, and longshore extended. In 1984, it has been extended again along the coastline, leading to protect 750 m of the coast. A first transversal groin of 108 m was installed in 1986, extended to 145 m in 1988, with the aim to reduce the rapid erosion of the beach in front of the riprap seawall. A second groin was installed 300 m southward, with the same extension, in 1994 (Figure 1b). The installation of these groins has not prevented the progressive erosion of the beach.. Recently, during the clustered storms of the 2013/2014, the sea front of Lacanau was massively damaged, and the pre-existent riprap sea wall was almost completely dismantled by the waves. The entire sea front was then redesigned and rebuilt, and the toe of the structure was moved seaward by 5–10 m along the 1.2 km of the current seawall. The seawall is relatively longshore uniform (Figure 3 see SEG 3 and 4) made up of a carapace of 1-3T limestone riprap resting on a filter layer and a geotextile.

A 3 m–wide foot stop allows the anchoring of the rock armor. This abutment is located between the altitude of 0.5 and 1.5 m NGF, but it does not rest on a hard substrate. The seawall is composed by a berm artificially covered by sand and a vegetated sandy slope on the crest. Further south, the seawall has the same dimension but slightly differ at the crest being backed by an artificial dune (Figure 3). Of note, this segment presents a shoreline oblique geometry design to smoothly connect the seawall to the downdrift coast.

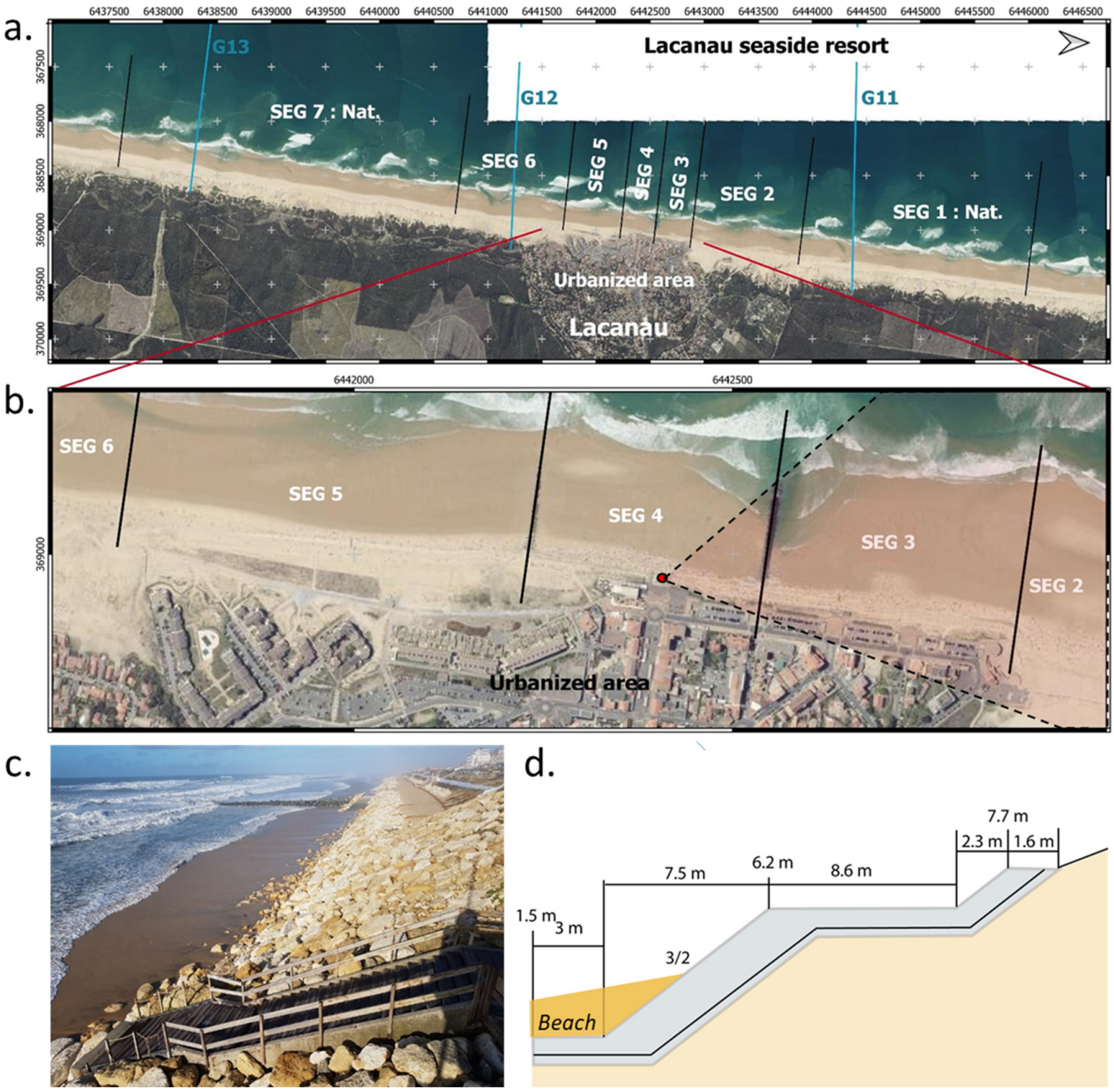


Figure 3. Longshore segmentation of the study area (**a**) SEG 1 to 7; blue lines indicate GNSS profiles. (**b**) Zoom at the urban area; the red point indicates the location of the photo, and the dashed black lines the field of view of (**c**) the photo of the seawall. (**d**) Schematic profile of the seawall.

Due to the meso–macro tidal range and large seasonal variability of beach shape, the seawall/beach relation is currently time-variable. Relatively to the Weggel classification [4] the interaction is alternately: Type III, "location of the seawall above mean high water and

below the still water line of storm surge", and Type IV, "within the normal tide range base is submerged at high water".

In terms of management, beach reshaping is carried out before the summer period, punctually before the year 2000, and then annually up to nowadays. In addition, after the strong erosion in 2014, a small artificial sediment supply (10^4 m^3) took place at the toe of the riprap seawall. These small-scale sand supply actions are assumed to have very temporary and local effects.

3. Material and Methods

3.1. Topo-Bathymetric Data

The analyzed dataset is composed by 7 airborne topographic LiDAR campaigns covering the beach and the dune of the entire study area (Figure 3a). Data were acquired in spring of 2011, fall of 2014 and then annually at the same period since 2016, and they were computed in 1 m spatial resolution grids DEM (Digital Elevation Model). The vertical error of the gridded LiDAR data was described in previous work [36] and shown for each LiDAR campaign standard error, between 0.15 and 0.08 m.

Additionally, since 2001, the beach–dune morphology was surveyed in autumn in 2001 and 2003, and then it was annually surveyed after the winter season, starting in 2006, at several transects within the study area (Figure 2). Surveys are realized by DGPS GNSS (RTK acquisition), with precision, and are about a few centimeters (always inferior to 5 cm) in both the horizontal and vertical coordinates. The beach–dune profiles are collected at low tide from the water line to the back of the dune in natural beaches up- and downstream and in direct adjacent sectors of the urbanized seafront (profiles named G11, G12 and G13, location in Figure 3). The surveys are focusing on beach evolutions with specific attention to systematically measuring micro-topography (e.g., beach scarp, berm and incipient foredune). The presented data are interpolated (1 m resolution), and they necessarily generate some errors. In a conservative consideration, this main error can be evaluated to be at maximum of about 0.10 m.

Bathymetric data were collected annually between 2017 and 2019 during the spring seasons (April) by the engineering office CASAGEC for the municipality in application of their management strategy plan. The survey was realized by using a single-beam echo sounder associated with a GNSS RTK solution coupled with an inertial SBG Ekinox station. Data were acquired following theoretical transects spaced 10 to 20 m in both longshore and cross-shore direction, covering the nearshore from 0.5 m to around 15 m in depth, covering a stretch of the coast of 4 km (1.5 km on both side of the urbanized seafront). Relative to the technical setting, the accuracy of the horizontal and vertical measurements is evaluated to be less than 5 cm, leading to a low implication of measurement error.

All data used (including topographic and bathymetric data) in the study are referenced in Lambert 93, NGF (Nivellement General de la France), official levelling network in Mainland France.

3.2. Longshore Segmentation

Along the Aquitaine coast, longshore variability of beach morphology and associated beach volume can be important due to the tridimensional inner and outer bar system imprint on the intertidal beach, as well as berm, which can be massive, highly dynamic and longshore irregular. In order to integrate natural longshore variability, the studied area was divided into seven segments of relatively homogenous characteristics (Figure 3). These segments are delimited considering beach–dune morphology, plus along the urbanized area, the type and geometry of the back beach geotechnical structures.

The extremal northern and southern sectors (SEG 1 and 7; Figure 3) cover 2.1 and 3.1 km of the study area, respectively. It is assumed that these two sectors are not significantly perturbed by the urban area and associated seafront management. These sectors are used as a comparison to evaluate the state of beach profile along the urbanized area and are defined below as "natural sectors". The urbanized area is surrounded by direct updrift and

down drift 1 km–long segment considerate as buffer (SEG 2 and 6; Figure 3). The urbanized area extends along 1.2 km and is bounded by a beach backed by seawalls. It is divided in three segments (SEG 3 to 5; Figure 3) relative to the geometry and the orientation of the seawall. Of note, the central segment (SEG 4) is bounded by two groins.

3.3. Cross-Shore Indicators

In line with previous works [35,36,47], the shoreline was defined as z = 6 m NGF, which roughly corresponds to the time and space averaged dune foot elevation along this part of the coast. This elevation was used to discriminate the beach from the dune compartment and to further compute the shoreline position (x_s). Beach–dune topographic profiles were extracted from each LiDAR grid, using 10 m–spaced profiles along the 15 km of the Lacanau coast (Figure 4). All profiles are extending up from mean sea level (MSL), corresponding to c. 0.5 m (Figure 5) and the dune toe c. 6 m.

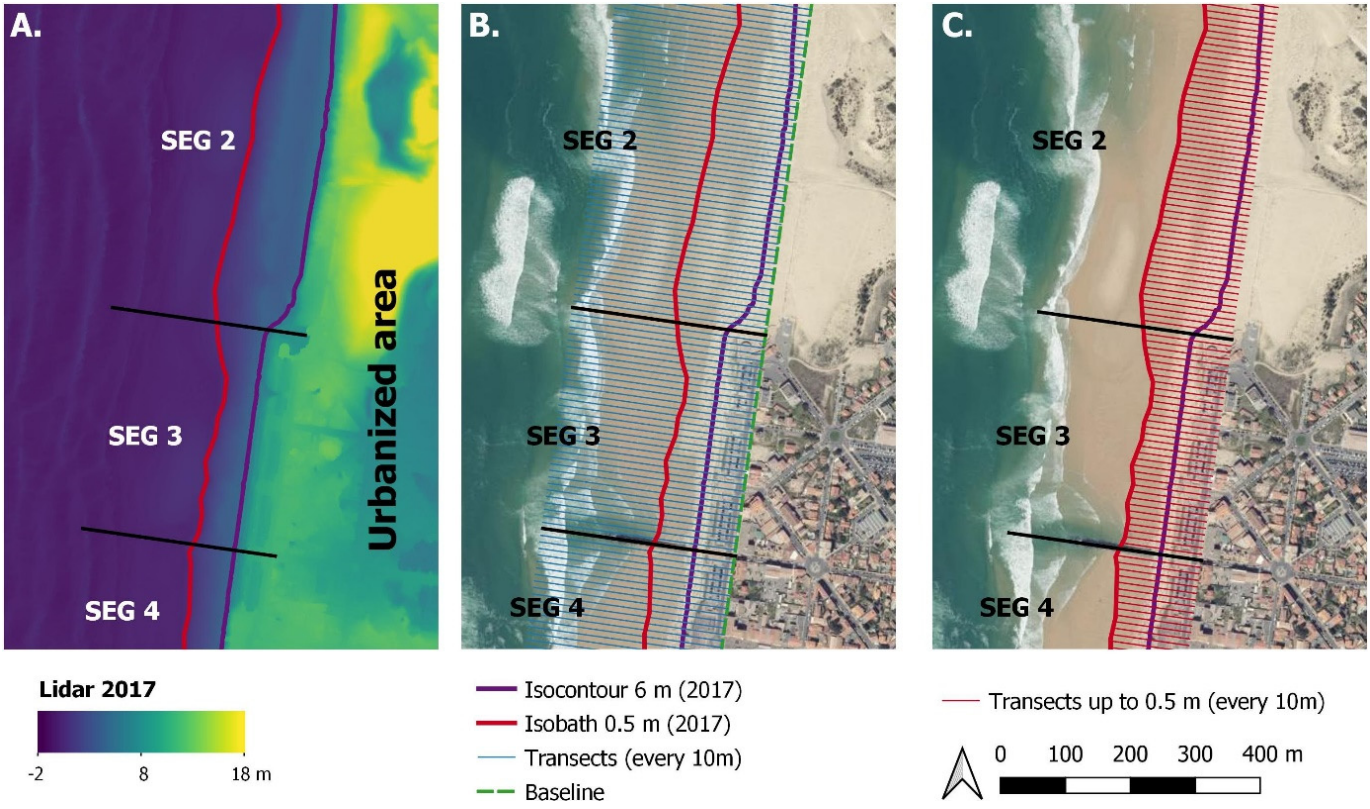


Figure 4. Steps of beach-dune topographic profiles extraction from LiDAR grids (zoom on segment 3). (**A**) LiDAR 2017 in this example, (**B**) 10 m-spaced profile and (**C**) extraction from 0.5 m NGF (mean sea level) to the dune. Red and violet lines indicate the 0.5 and 6 m NGF contours, respectively.

Given the broad changes in both time and space of the beach–dune profiles, data are considered in two references: (i) data are regarded in classical geographic coordinates and (ii) a local reference frame is used secondly. For each beach–dune profile, the data were translated in order to get the same origin (x = 0). This local cross-shore position systematically corresponds to the intersection of the beach–dune profile with the shoreline (z = 6 m NGF, Figures 5 and 6a). For each segment, beach profiles were stacked to obtain a beach envelop (Figure 7a,d,g), and a mean profile per year was further computed (Figure 7b,e,h). This local reference frame is more suitable to compare beach-profile shapes and envelopes.

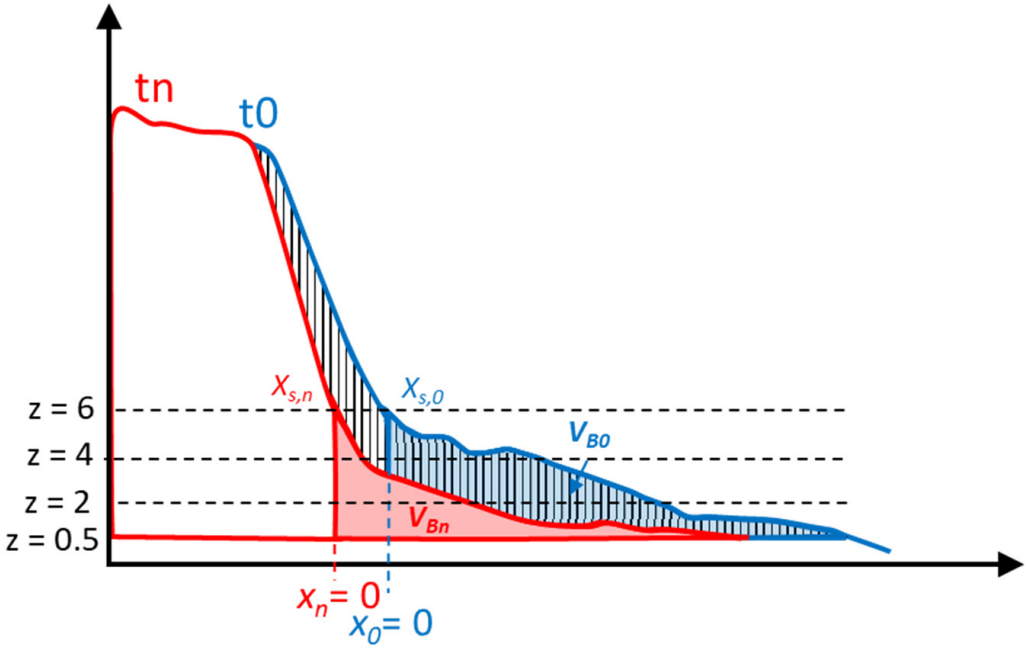


Figure 5. Schematics of the beach–dune profile analysis at a given transect: shoreline position (x_s) and beach volume (V_B) between z = 0.5 m and z = 6 m. In order to compare beach–dune profile shape in both time and space (see Figure 4), a local reference frame is used in which, for each profile, x = 0 is defined as the intersection of the beach-dune profile, with elevation z = 6 m.

The beach volume (V_B) is defined as the sediment volume between the profile intersections with the MSL (0.5 m NGF) and 6 m NGF in m^3/mL. For each individual beach profile, the V_B is calculated. Mean and standard deviation volumes are computed based on the distribution of individual V_B values per segment. Inter-annual V_B changes were also computed and were defined as the differences in absolute value between two successive annual surveys. In the urban area, where the seawall is backing the beach, the form and extension of the seawall is integrated into the profile. The volume corresponding to the extension of the structure is estimated at 19 m^3/mL relative to the structure geometry (Figure 3d) and is subtracted to the total beach profile volume. Note that sediments or substrate below the observed envelop cannot be considered systematically mobilizable. However, this estimate, which can be calculated homogeneously for each of the measurement campaigns, allows the relative comparison of the sand stocks positioned on the beach and the characterization of their dynamics (inter-annual and seasonal variability).

Note that LiDAR, GNSS and bathymetric echo-sounder data present a statistical relative error (error always positive) always smaller than 0.15 m in the Z coordinate. The absolute error used to be compensated, and the residual is close to 0 (no systematic bias was detected in the analysis for any campaign). Thus, we assumed that the repercussion of vertical error on beach volumes evaluation and topographic proxies location is very low and can be evaluated qualitatively to a few cubic meters per linear meter (m^3/mL) and less than 2 m in horizontal coordinate, respectively; this is not significant in comparison to typical observed beach volumes' and topo-bathymetric contours' evolution at the study site.

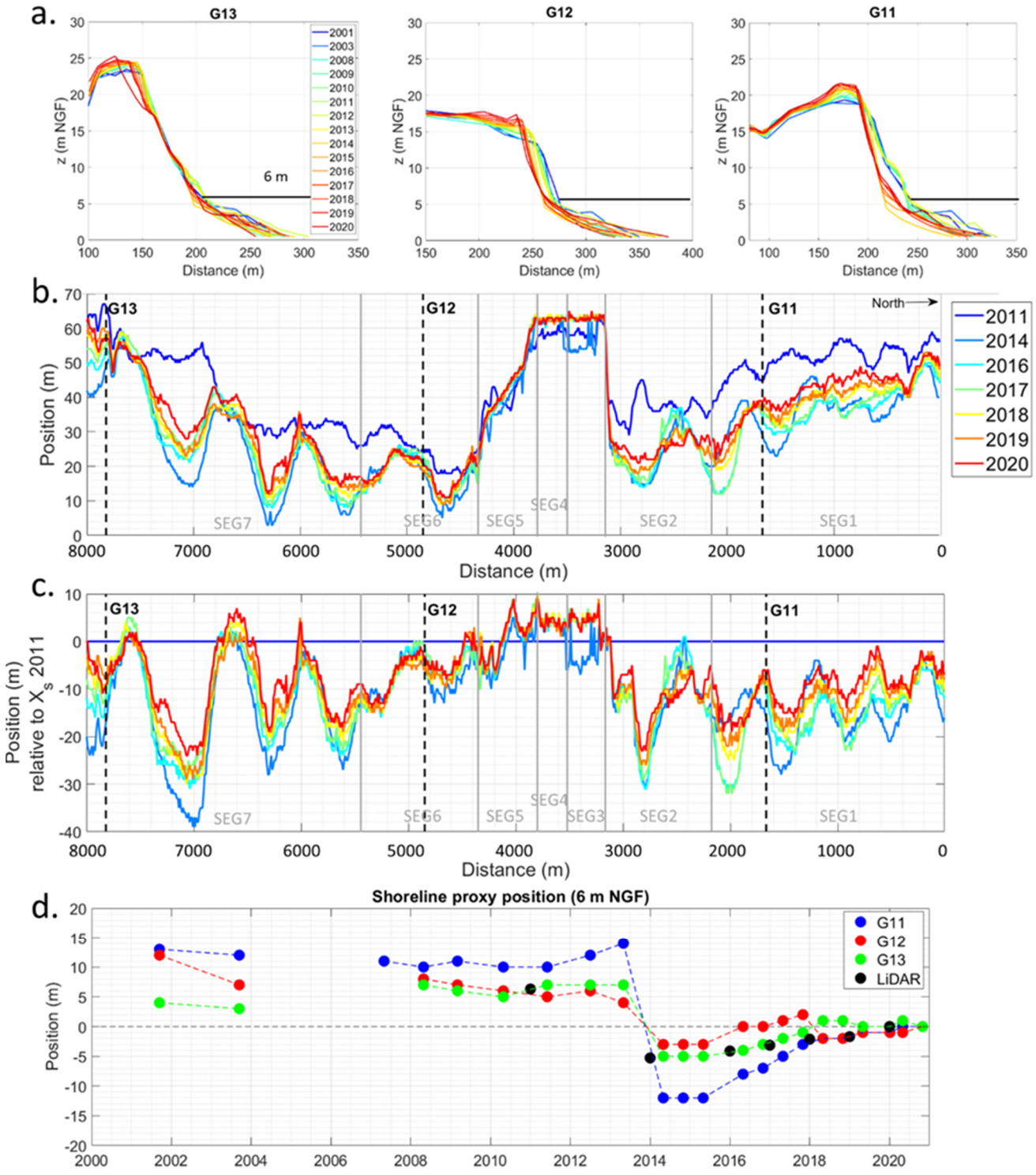


Figure 6. (**a**) DGPS annual evolution of beach-dune profile between 2001 and 2020 (location of each transect is reported in panel b, (**b**) LiDAR derived shoreline position (x_s) along the study site between 2011 and 2020, (**c**) LiDAR derived shoreline position (x_s) relative to 2011 shoreline position and (**d**) shoreline position x_s (6 m NGF) relative to 2020 shoreline position at the 3 DGPS transect and averaged along the study site (LiDAR data).

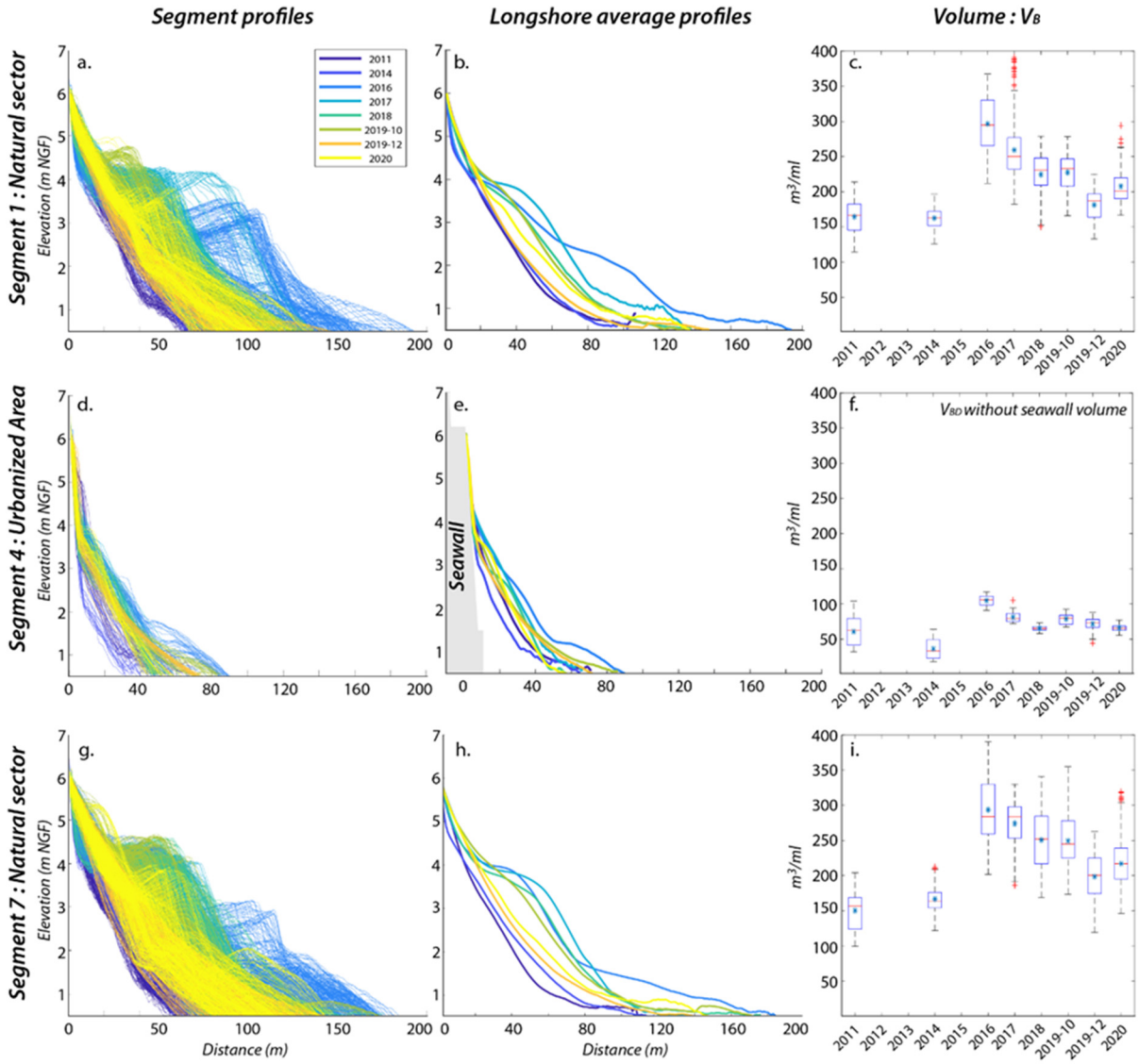


Figure 7. Beach morphology and associated volumes per year for the period 2011–2020 of (**a**) all LiDAR beach profiles stacked, (**b**) longshore average profiles and (**c**) box plot of beach volume V_B for the northern natural segment (SEG 1). (**d**–**f**) Same organization for the central urbanized area (SEG 4) and (**g**–**i**) the southern natural segment (SEG 7). For the box plots, the central horizontal marks in the box plots indicate the median, and the top and bottom edges of the blue boxes indicate the 25th and 75th percentiles, respectively. Maximum whisker length extends up to 1.5 times the interquartile range, and the outliers are plotted individually using the "+" symbol.

4. Results

4.1. Decadal Evolution of Shoreline Position

Over the last 20 years, the shoreline position (x_s) at the three transects (G11 to G13; Figure 3) has retreated from 4 to 13 m (Figure 6a). Between 2001 and 2013, x_s was barely stable, except for the nearest transect of the urbanized sea front (G12). An important retreat is observed after the 20132014 winter events, with local retreats ranging between 7 and 26 m.

Complementary, between 2011 and 2014, LiDAR data show that the x_s longshore average retreat is about 14.5 m at the north of the seawall (SEG 1 and 2) and 12.9 m at the south (SEG 6 and 7). Large alongshore variability is observed related to almost symmetric

beach–dune megacusps erosion patterns, ranging from 400 to 800 m large and reaching 20 to 40 m in amplitude (Figure 6b,c).

Between 2014 and 2018, the entire stretch of the coast shows significant recovery in average 1.8 m at the north and 4.1 m at the south of the seawall (Figure 6), but at local variable rhythm, with sand accumulation being larger in the cusp embayment relative to the horns. The 2018/2019 winter was the second more energetic of the last 20 years (Figure 2) and induced a new shoreline erosion, mostly observed at the horns of the preexistent cusps (see Figure 6c, at x = 2500, 5000, 6500 or 7500 m). However, this winter has finally a low impact on the shoreline alongshore average position, and, in fact, during the 2014–2020 period, the shoreline recovered 4.3 m and 6.7 m at the north and the south of the seawall, respectively. The shoreline retreat observed in 2014 was approximately half reduced in the megacusp embayment.

4.2. Beach Shape and Volumes

The general characteristics of beach morphology and associated average beach volumes (V_B) are similar upstream (SEG 1) and downstream (SEG 7) of the urban sector of Lacanau, with V_B = 215 and 225 m^3/mL respectively. The variability in space of the V_B expressed by σ V_B is also similar, between 16 and 43 m^3/mL and 19 and 46 m^3/mL for SEG 1 and SEG 7, respectively (Table 1 and Figure 7a–c,g,h,l). At the center of the urban area (SEG 4; see Figure 7d–f), the alongshore average V_B is substantially reduced (71 m^3/mL, or 68% lower) compared to the natural segments (SEG 1 and SEG 7). Along the walled backed beach, the same lower availability of sediments is noted for SEG 3 and SEG 4, while the V_B values are slightly higher along SEG 5, due to the shoreline oblique geometry of the seawall (Table 1).

Table 1. Longshore averaged beach volume (V_B in m^3/mL) per segment and per year at Lacanau. The minimum and maximum volumes per segment estimated per segment are highlighted in light and dark gray, respectively.

V_B: m^3/mL (σ)		2011	2014	2016	2017	2018	2019 Oct.	2019 Dec.	2020	Mean V_B
SEG 1	***Natural***	165 (*25*)	163 (*16*)	297 (*39*)	259 (*43*)	225 (*32*)	227 (*28*)	181 (*21*)	208 (*23*)	**215**
SEG 2	***Transition***	172 (*26*)	152 (*9*)	196 (*33*)	264 (*37*)	226 (*27*)	242 (*27*)	200 (*25*)	240 (*34*)	**211**
SEG 3		79 (*19*)	73 (*23*)	72 (*9*)	93 (*19*)	95 (*18*)	82 (*7*)	60 (*9*)	37 (*24*)	**74**
SEG 4	***Urban***	61 (*21*)	36 (*15*)	105 (*7*)	81 (*8*)	65 (*4*)	79 (*8*)	72 (*10*)	66 (*6*)	**71**
SEG 5		99 (*28*)	53 (*28*)	139 (*38*)	141 (*38*)	119 (*32*)	106 (*49*)	78 (*31*)	80 (*31*)	**105**
SEG 6	***Transition***	153 (*11*)	149 (*21*)	291 (*45*)	224 (*21*)	248 (*44*)	221 (*18*)	180 (*24*)	220 (*44*)	**211**
SEG 7	***Natural***	150 (*25*)	167 (*19*)	293 (*46*)	274 (*34*)	251 (*39*)	249 (*39*)	198 (*35*)	217 (*35*)	**225**

This difference of V_B between urban and natural segments is more pronounced before the winter period, when sediments are generally much more abundant on the beaches. The deficit of V_B on the urban sector compared to the natural sectors is then 69% against 62%, respectively, before and after the winter (Table 1).

The variability of the envelope is also greatly reduced in the urban area compared to the natural areas; this is mainly because no summer berm is observed, contrary to adjacent sectors (Figure 7). Indeed, SEG 4 exhibits a flat beach with very reduced variabilities (σV_B: 4 to 21 m3/mL, generally >10 m^3/mL), in comparison with natural sectors (σV_B: 16 to 46 m^3/mL; see Table 1).

In 2020, the V_B values of the natural (SEG 1 and SEG 7) and transition segments (SEG 2 and 6) are close to the 2011–2020 average values. In contrast, in front of the seawall (SEG 3, 4 and 5), the V_B is substantially lower than in the previous years. This is particularly true at the northern part of the seawall (SEG 3), where the V_B is the lower volume observed of the period (37 m^3/mL; Table 1), due to the presence of a rip channel almost positioned at the seawall toe.

4.3. Longshore Beach Variability: Unwalled vs. Walled Beach

In order to analyze the evolution of V_B in natural area ($V_{B\ Nat}$) with volume in the urban sector ($V_{B\ Urb}$) during the 2011–2020 period, results for SEG 1 and 7 are merged (Figure 8a). The ratio $V_{B\ Urb}/V_{B\ Nat}$ highlights the relative variation of sediment volume between the two sectors. It shows that the weak availability of sediment, as well as the decrease in sediment volume in front the seawall, seems relatively progressive (linear) and continuous over the studied period, from 44% in 2011 to 24% in 2020 (Figure 8a). Note that there is no substantial decrease between 2011 and 2014, but it necessary to consider that LiDAR in 2011 was surveyed in March (post-winter), whereas, in 2014, the survey occurred in October (post-summer). In fact, in 2014 the profiles (volume) at the end of the summer period (recovery period) are barely identical to those observed after the winter. In other words, after a season of recovery, the beach still had winter characteristics.

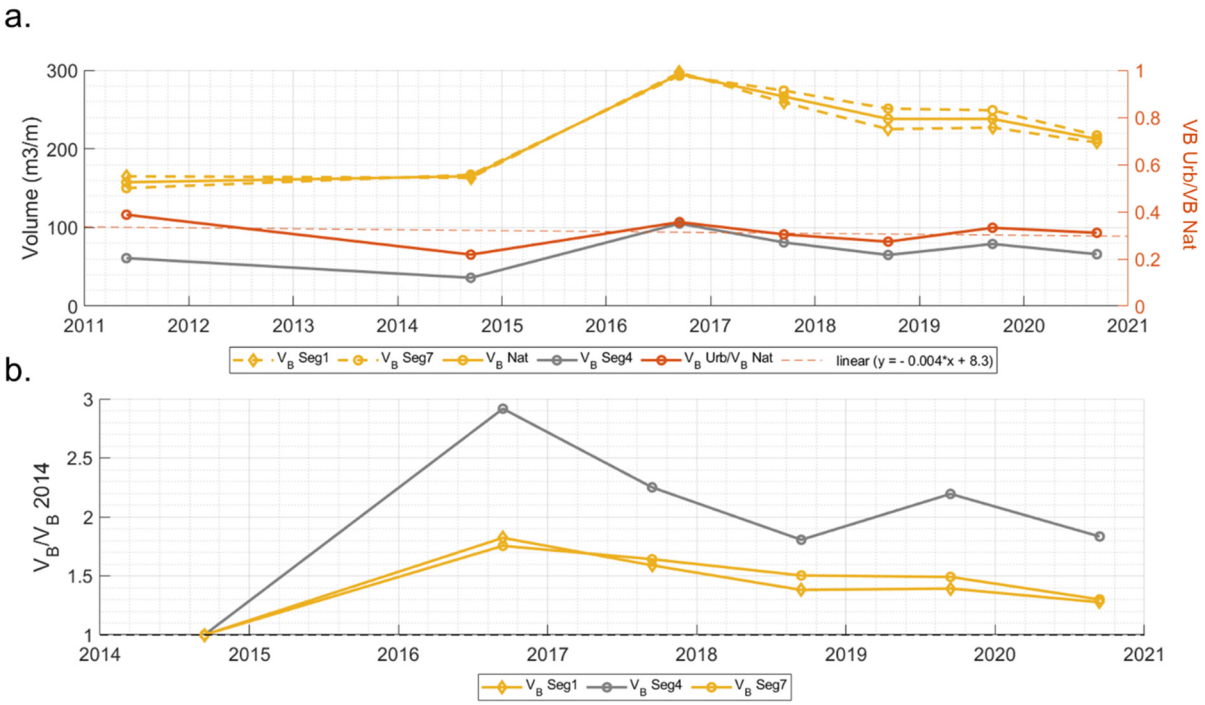


Figure 8. Evolution of longhore average, V_B, for natural (SEG 1 and SEG 7) vs. urbanized segment (SEG 4) (**a**); the reference for ratio $V_{B\ Urb}\ /V_{B\ Nat}$ is the right axis. Evolution of V_B on the same segments relative to V_B 2014 (**b**).

Even if V_B is decreasing in front of the seawall, inter-annual variations are broadly similar to those observed for the northern and the southern natural sectors, especially since 2014 (Figure 8b). Except between 2011 and 2014, where sediment volumes are stable within the natural segments, while a substantial decrease of V_B is observed in front of the walled sector (attributed to a relative higher impact of the 2013/2014), evolution tendencies are roughly similar. For the entire study area, both in urbanized and natural sectors, V_B increased between 2014 and 2016 and has decreased continuously since 2016.

Finally, between 2014 and 2020, V_B increased, on average, by about 55 m^3/mL on natural segments, whereas it has decreased about -18 m^3/mL on the seawall backed beach. Note that the 2011 survey was performed during spring, whereas the 2020 survey was in autumn. Considering that the seasonal variability of the beach–dune volume is, on average, about 74 m^3/mL [41], we can reasonably consider that, in 2020, the V_B at natural segments is similar to the situation in 2011. This is not the case in front of the seawall, where a benefit of post-2013/2014 recovery is no longer observed and where V_B notably decreased. It should be noted that no perturbations of the natural segments (downstream compared to upstream) are attributable to the presence of the seawall. Indeed, a similar

V_B and evolution were observed during the studied period for the two natural segments (see Figure 8).

5. Discussion

The impacts of different kind of built structures on beach morphology and erosion hazard are theoretically well-known (Figure 9; see References [1,2,13,48,49]), but, in fact, magnitudes of the perturbations are related to multiple and complex non-linear factors. In the literature, conclusions appear often discordant, site-dependent and strongly related to the approach taken (flume experiment, model and field observation).

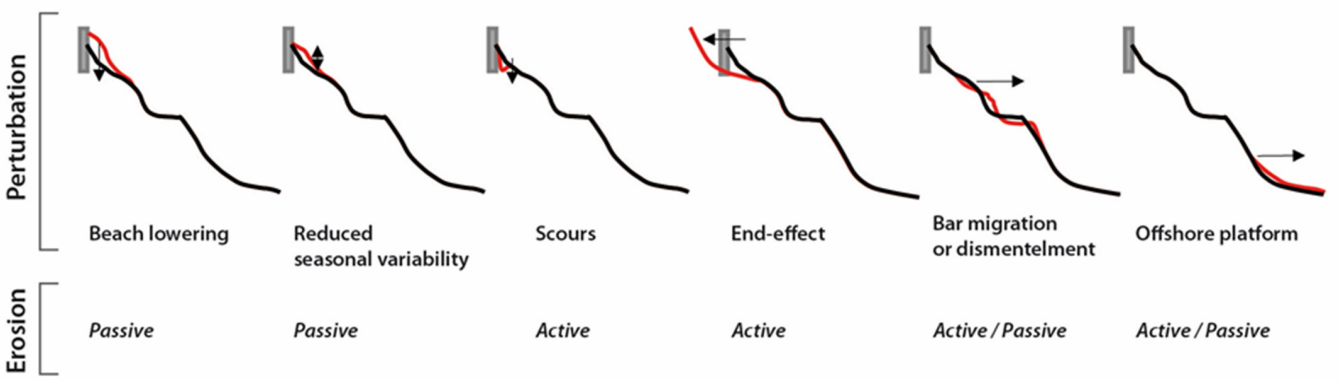


Figure 9. Schematic illustration of passive and active seawall-induced morphological perturbations reported in the bibliography.

Adverse effects attributed to the seawall on adjacent beaches are multiple and can be evaluated through several topo-bathymetric indicators: (i) end-effect [20,21,50,51], affecting the shoreline position; (ii) beach lowering [52–54], affecting the beach level and morphology directly in front of the wall; (iii) temporary [10,19] or persistent scours or troughs [55–57], affecting the bathymetry in front of the wall; (iv) offshore bar migration, affecting the nearshore bar form and position [57,58]; or (v) offshore sediment redistribution, generating an offshore flat plateau [10].

The assessment of seawall-induced perturbations generally suffers from confusion related to the absence of distinctions between active erosion (topo-bathymetric perturbations generated by the structure) and passive erosion (long-term shoreline evolution context [22,23,29]. The anticipated adverse effects related to seawalls (previously cited) are regarded below, assuming that the studied dataset can support conclusions on multi-annual-to-decadal evolutions caused by the presence of the seawall.

5.1. Beach and Shoreline Perturbations Associated to the Structures

The main adverse impact assignable to active erosion is the end-effect, which is observable at the both sides of a seawall. End-effects were mainly argued to be caused by the reflection and diffraction of waves at the ends of walls, concentrating wave-induced energy, generating rip currents and seaward return flows [20,50]. Other processes are proposed, such as sand trapping [3], groin effect [16] or headland effect [22], but these are not relevant in our context. Perturbations affecting the beach and the shoreline position directly at the downstream end of the wall are often reported to extend from 50 to 300 m [16,20,21,51]. The relation between the magnitude of the perturbation and seawall length was investigated in the bibliography, but the laboratory and field data show no consistent results [14], and for long seawalls, no correlation is physically plausible [22]. This is in contrast to other management solutions for which direct relations are observed; see Reference [59], for example. At the Lacanau seaside resort, a local retreat of approximately 5–10 m along 400 m is observable in 2011 at the southern end of the seawall (Figure 6b) relative to the longshore average position of the shoreline. Less clear perturbation is observable at the north end, with a 5 m retreated shoreline position along 200 m.

These impacts attributed to the seawall can be considerate as relatively small regarding the fact that this coast is dominated by highly energetic conditions and comparing with observed impact of storm-induced erosion. In addition, no clear accentuation of the shoreline retreat is observable after a massive erosion sequence (2013/2014 winter; Figure 6b,c). After these storm events, megacusps at the strictly adjacent sectors to the wall have similar (or reduced) dimensions in comparison with those observed along the rest of the coast. In 2020, the local end-effects appeared to be reduced, considering the shoreline proxy (dune foot) or lower topographic contours (see Figure 10), concluding that potential upstream and downstream end-effects at a Lacanau site are mostly temporary. For today, potential adverse end-effects have similar dimensions to the mega cusps observed within the studied area and are compensated by highly dynamic sediment circulation, sediment availability and moderate management actions (i.e., beach and dune reshaping or sand supply). Limited adverse effects are also related to the specific geometry of the seawall, for which the southern part is composed of a shoreline oblique segment (SEG 5) for the very purpose of reducing the perturbation.

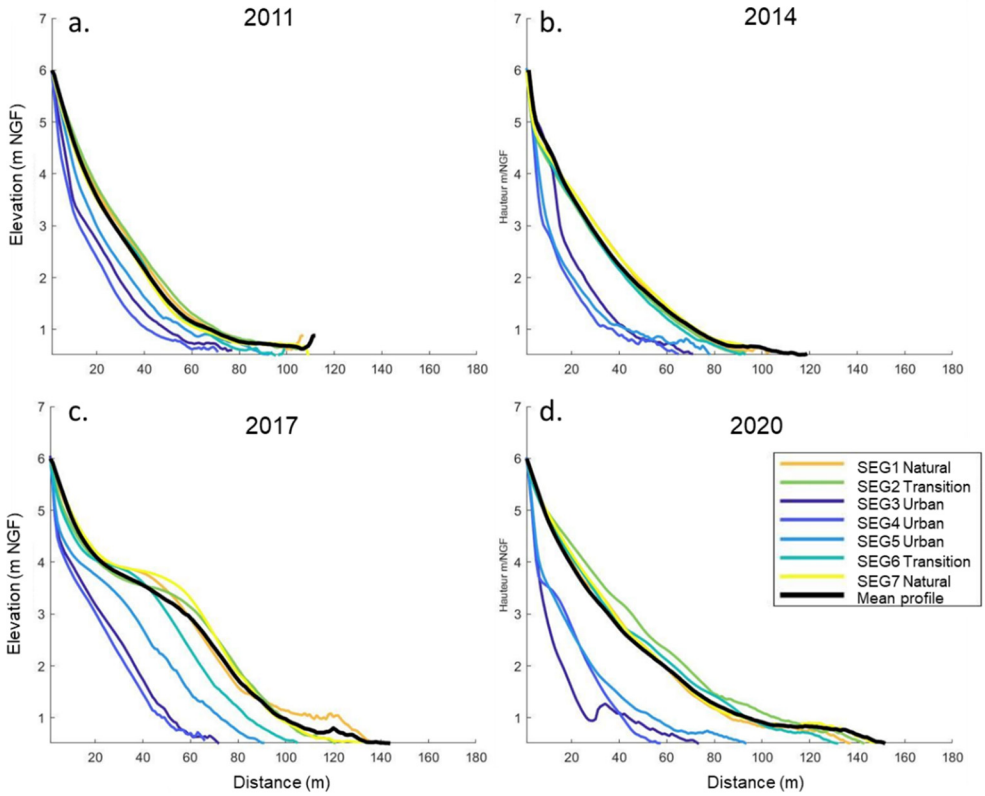


Figure 10. Alongshore average beach profile per segment (**a**) in 2011, (**b**) in 2014, (**c**) in 2017 and (**d**) in 2020.

At a larger scale, Figure 11a shows that the Lacanau sea front is located approximately at the center of a persistent shoreline deviation of wave length of c. 8 km. This deviation of the shoreline was already detected before the installation of the seawall (in 1966) and has approximately the same amplitude (between 30 to 35 m) as thought at the time. Here, it is assumed that there is no link with the presence of the seawall. The nature of this large-scale shoreline oscillation, which can play a role in the future evolution of the shoreline at the study site, is not clearly known and should be further investigated relative to chronic erosion hazard and impact of sea-level rise.

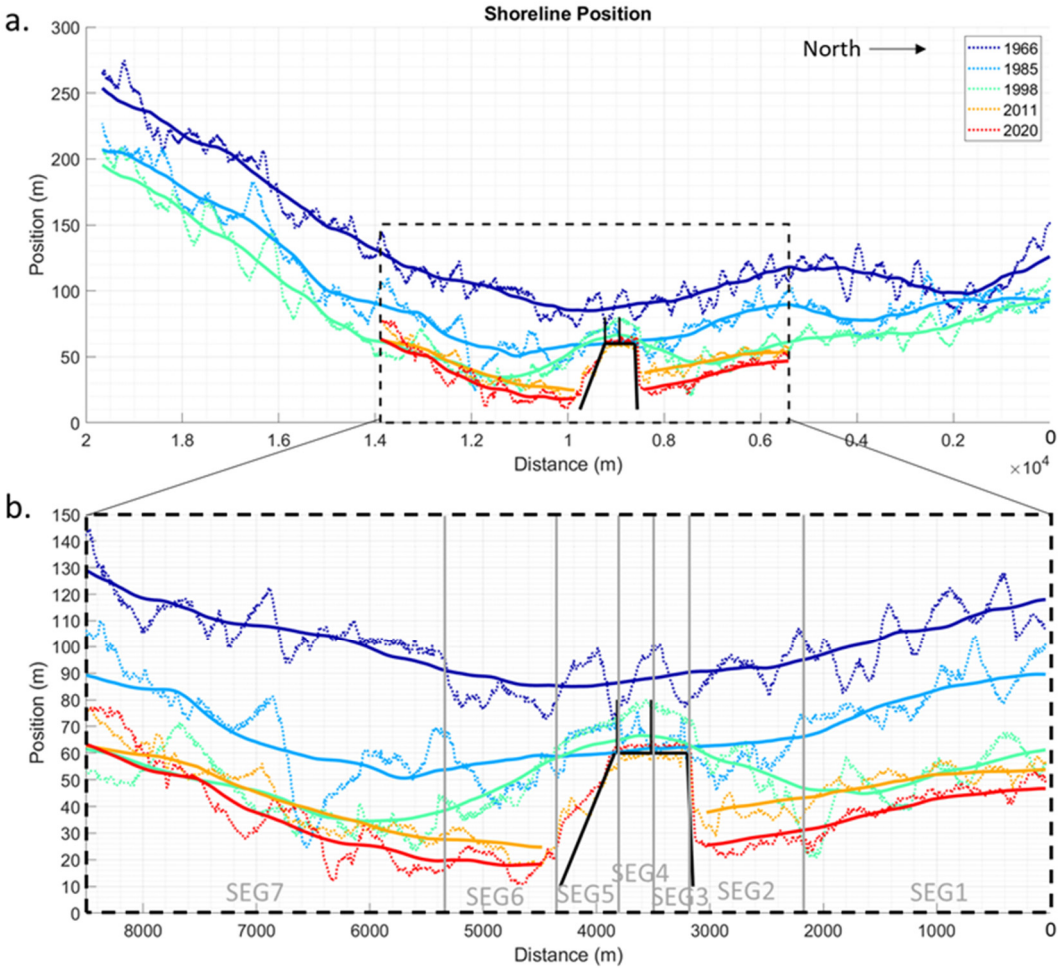


Figure 11. Shoreline position (x_s) relative to a rectiligne baseline: (**a**) along 20 km and (**b**) zoom along the study site from 1966 to 2020. Solid line is the shoreline centered moving average, calculated over a sliding window of 2 km. Black line indicates the position and the geometry of the seawall and the groins.

Seawalls are also commonly blamed for generating beach lowering; see References [52,54] for examples. These perturbations are reported to be related to a combination of cross-shore-dominated processes associated with wave reflection [55,60,61] combined with a gradient of longshore current [10,19,62–64] affecting the beach and extending to the nearshore area. Beach lowering, relative to adjacent sector, is generally associated with the faster establishment of a flat beach profile in winter (i.e., during fall) and reduced seasonal variability in beach volume between the summer and winter seasons [53].

At Lacanau, low beach and reduced seasonal variability are obvious and are mainly a manifestation of passive erosion due to the general shoreline retreat and relative progressively more seaward position of the seawall (Figure 11). The first qualitative observations of beach lowering at the site were reported in 1998 [40]. In fact, with reference to these data and specifically the shoreline position in 1985 (Figure 11), it can be supported that the lowering of the beach had already started by then (probably as soon as the first installation of seawall during the 1970s). Our comparison of mean cross-shore profiles in an urban sector backed to the seawall (SEG 4) with those in natural sector (without seawall, SEG 1 or SEG 7; Figure 7) shows no significant additional active erosion at the toe of the seawall (scours); the upper part of the beach between is notably steeper (c. 10% against 5 to 6% for natural beach), but the lower part of beach profile (beyond 1 m) in front of the seawall is roughly similar to the profile of adjacent beaches.

5.2. Impact on Nearshore Bathymetry

Seawall-induced perturbations on the nearshore bathymetry are supposed to be signs of active erosion caused by wave reflection and perturbation of the longshore current, first affecting the beach extending to the nearshore area. At the study site, between 2017 and 2019, no major scours were usually observable, and no significant or persistent lowering of the lower part of the beach was noticed in front of the wall (Figure 12a). The position of the 0 m isobath shows a reduction of the beach width at the northern part of the wall, but no similar pattern is observable at −2 m (Figure 12b). Interestingly enough, no clear bathymetric perturbation can be associated to the two groins, indicating that their role of capturing sediment is weak and intermittent. In fact, the groins fail to retain sand in the long term, mainly due to the large tidal range, which periodically allows the groins to be by passed at low tide and passed over at high tide.

As reported in several field studies, scours are not necessary observed at seawalls [19,23,53]), including after storms [6]. Four reasons are proposed to explain the absence of scours (active erosion) or more generally reduced erosion pattern along Lacanau sea front, the two first ones relative to the seawall (intrinsic): (i) the position of the seawall relative to the beach. In fact, the toe of the seawall is affected by the runup only during few hours (high tide) at time scale of day during spring tide or storms. This is limiting the time of direct interaction between waves and the wall; (ii) the type of seawall (riprap seawall), which are promoted to limit wave reflection and thus induced perverse effect. The two others factors are relative to the hydro-sedimentary context (extrinsic): (iii) the meso–macro tidal range at the site associated with a very high annual littoral drift rate (local mean residual longshore drift of c. 300.10^3 m^3/yr, [65]), which supports permanent cross-shore/longshore sediment redistribution. This is a factor in permanently smoothing out or filling in any such local scour at the beach and the nearshore; (iv) the relatively high sediment availability within the coastal system. In fact, despite the context of chronic erosion over the long term, beaches at the North of the study site are wide and beach volume are substantial [38]. The very high annual littoral drift rate naturally brings large sand supply, conferring a strong capacity of recovery of the beaches on a seasonal and multiannual time scale.

Some studies with contradictory results have related the potential modification of nearshore bar position or form to the presence of seawall [57,58]. At Lacanau, the positions of the isobaths—−2 to −10 m do not highlight any clear wall-induced pattern associated with the presence of the seawall. Slight differences in 3D rhythmic patterns can be noted in front of the seawall, compared to the adjacent sector (more longshore uniform outer bar, Figure 12a; or more pronounced trough, Figure 12b,c). However, this observation cannot be conclusive relative to the strong spatiotemporal variability of the inner/outer bar pattern and the fact that surveys were realized annually at spring, preventing the detection of perturbation on seasonal variability. A bathymetric survey should be pursued in order to confirm potential multi-annual trends, and, eventually, analyses of seasonal perturbation should be performed, particularly at the outer bar location and beyond the theoretical depth of closure.

Finally, concerning offshore sediment redistribution, studies based on flume experiment [10] or using parametric models [14,15] have shown that taking sand from the beach in front of a wall and moved offshore formed a relatively flat plateau that extended the offshore breaking zone. Based on the formula proposed in References [66,67], the depth of closure at this coastal site is estimated to be between 15 and 20 m depth. Unfortunately, the available bathymetric surveys are limited to a c. −17 m depth, preventing them from being totally conclusive. However, these results are interesting enough, considering that, over the three years of bathymetric survey, nearshore bathymetric perturbations between a depth of 0 and 15 m are mostly subtle, and the 15 m–deep isobaths exhibit persistent oscillation with an amplitude of a 20 to 60 m, roughly in front of the seawall (Figure 12d). As for the outer bar form and position, further monitoring must be conducted to conclude on the nature of these oscillations and if a link can be supported with the presence of the seawall.

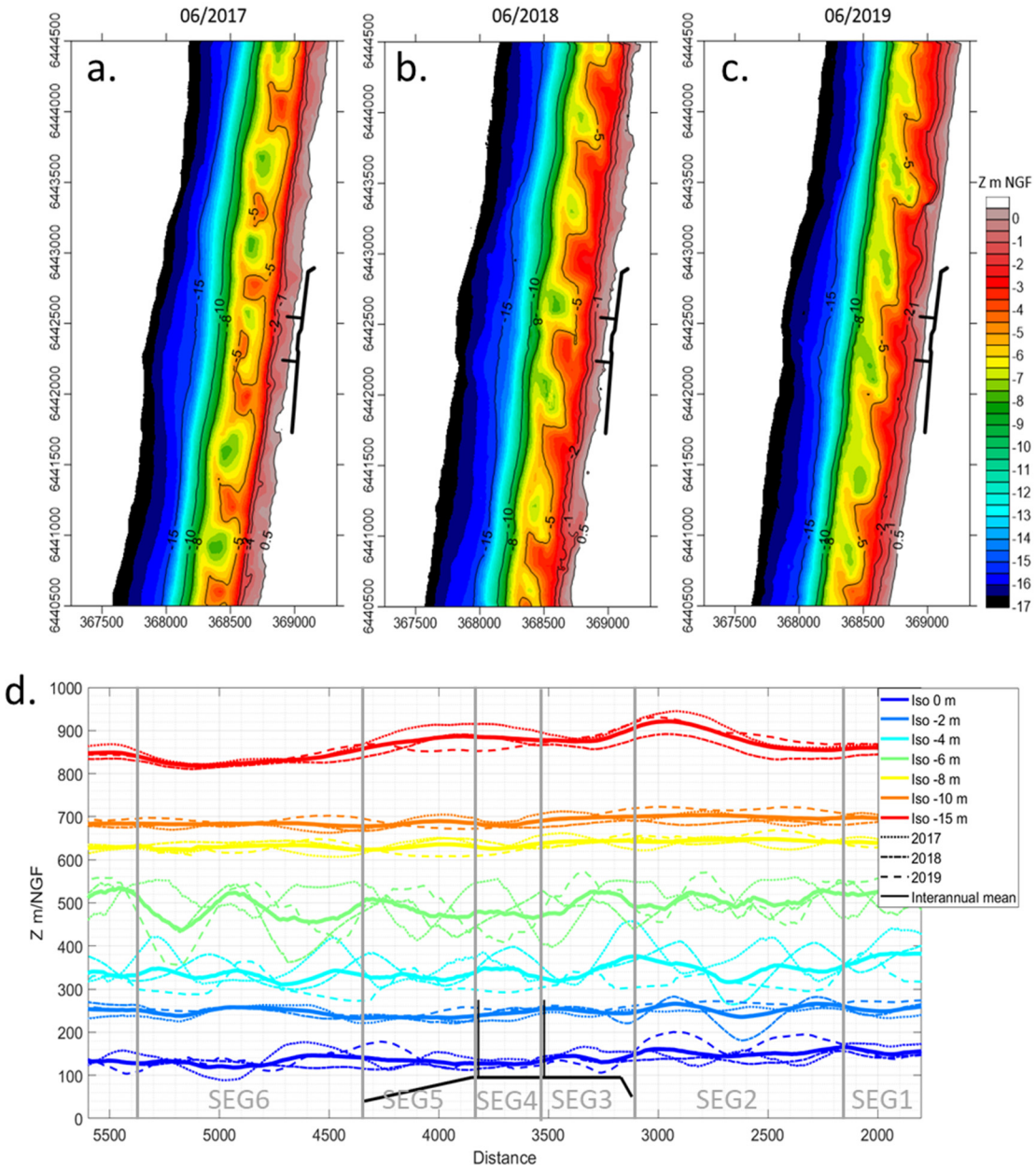


Figure 12. Annual DTM of nearshore bathymetry at the center of the study site (period 2017–2019) (**a**–**c**), and superposed isobaths position for each survey and time-averaged isobath position relative to a rectiligne baseline (**d**). Black line on the plot indicates the position and the geometry of the seawall and the groins.

5.3. Recovery and Accommodation Space

At the Lacanau site, a small long-term seawall-induced effect on topo-bathymetry was observed; this is in line with several studies realized on highly energetic coasts, e.g., in California [6,30] or Oregon [68,69]. The reduction of the beach in front of the seawall is due to the general long-term chronic shoreline erosion along this stretch of the coast. Shoreline retreat is characterized by successive episodes of mega cusp erosion potentially with a large amplitude, similar to that observed after the 2013/2014 winter [34,36] or that previously observed in 1979 [70]. Subsequent periods are marked by progressive erosion at the horns of the cusp during moderate to highly energetic winters and substantial accumulation of sand in the bay during summer (Figure 6b). After 6 years (2014–2020), the shoreline position in the mega cusps was offset by half and the shoreline tends to be realigned, resulting in a net

landward longshore average translation of about 10.2 m at the north of the wall (SEG 1 and 2) and 6.2 m at the south (SEG 6 and 7) between 2011 and 2020. In the cusp directly adjacent to the wall, relative beach recovery is globally similar to the rest of the coast (Figure 6b,c, Figures 10 and 11). Results show that extreme storm events (winter 2013/2014) can be responsible for 30-to-40 m local shoreline retreat (Figure 6), with the alongshore average retreat being higher than 10 m at the timescale of a winter. The shoreline retreat relative to the 1966 alongshore average shoreline position was about 66 m in 2020 (1.2 m/year). Considering that, in 2020, the mean width of the upper beach in front of the wall (between Mean Higher High Water and the seawall toe) was around 30 m, the disappearance of the dry beach (i.e., backshore) in front of the seawall will take place anyway within 20 to 25 years within the current seawall geometry (due to global shoreline retreat). This is not considering a potential extremely erosive winter, which could be responsible to sudden degradation of the situation (Figure 13a).



Figure 13. Aerial photographs of Lacanau from the south (**a**) after last storm of the winter 2013/2014 on 03/2014, showing the severely damaged sea defenses and mega cups erosion pattern (photo: Julien Lestage); and (**b**) 2-and-half years and after, showing the new configuration of the seawall and the recovery at the beach–dune interface (photo: Jerome Augereau).

As observed in the 2020 survey, due to the actual position of the sea wall within the beach profile, the common nearshore bar-rip channel dynamics can temporally but substantially reduce the beach width in front of the seawall and eventually promote damage to the seawall (Figure 10d). Future disappearance of the dry beach will drastically modify the hydrodynamic conditions at the base of the wall. Conclusions drawn here of no significant active erosion caused by the seawall could then be questioned.

Finally, a few quantitative approaches are available to anticipate the topo-bathymetric impacts of sea walls [13]. Promising works were recently presented [14,15] to draw expected perturbations related to seawall and sea-level rise on nearshore topo-bathymetric profiles. These parametric models should be interesting to set up on the study site in order to address questions of acceleration of beach disappearance, modification of the bathymetry or potential drastic increase of perturbations of longshore sediment transfer.

6. Conclusions

Hard coastal structures are usually thought to perturb hydrodynamic conditions and sediment exchange within the coastal system, leading to adverse effect. There is no consensus in the literature on the impact of seawalls, eventually because in situ long-

term evolution depends on many factors, including the position of the wall relative to the adjacent coastline, geometry and materials, ground water dynamic, tidal range, wave energy, sediment supply and management actions. Thus, the negative effects reported in the bibliography are not systematically generalizable.

Classically reported perturbations associated with seawalls were analyzed at Lacanau sea front, thanks to an extensive topo-bathymetric dataset acquired within two decades. The most dramatic manifestation of the presence of the seawall is the beach lowering and the reduction of beach variability at the seasonal and interannual timescales in front of the seawall. This manifestation of passive erosion is related to the context of chronic shoreline retreat at least since the mid of the 20th century, preexistent to the construction of the seawall. The shoreline is retreating by erosion/recovery cycles characterized by (i) mega cusp erosion, (ii) mega cusp progressive infilling (recovery) and (iii) longshore non-uniform realignment (horn retreat) during subsequent winters. After the extremely energetic 2013/2014 winter and subsequent years, no evidence of an increase of erosion or slowdown of recovery related to the presence of the seawall is observed at direct adjacent sectors. The only perturbations directly attributable to the seawall (active erosion) are relatively small, only limited to temporary end-effect, potential slight perturbation of outer bar pattern and the setup of a slight platform at the deeper part of the profile. To date, there is no evidence that the seawall has produced non-reversible adverse effects, mainly thanks to the highly dynamic hydro-sedimentary conditions (tidal range, wave induced longshore drift and high sediment availability) promoting permanent sediment redistribution within the coastal system.

The choice of implementation of coastal structures always needs to be carefully regarded, considering positive effect in regard to perturbations, including local and immediate, as well as extended and long-term, adverse effects. Another point to consider relative to the future consequence of climate change is the possibility of maintaining or dismantling such solutions. As in many urbanized coasts worldwide, the sea-level rise and modification of storm regime associated with chronic shoreline erosion will lead to new modes of interaction between hydrodynamic conditions and the structure probably modifying morphodynamic response of the nearshore system. On these coasts, the reflection about occupation mode within coastal management plan for the next decade is at a turning point. In most cases, to respond at the increase of hydrodynamic stresses on structures, the chosen path is to hold the line and reinforce structures (i.e., seawalls). When there is no obvious disturbance of the hydrosedimentary functioning of the coastal system, another approach is possible. Accepting a rapid realignment of the coastline relative to the adjacent sectors, the renatualization of the shoreline can be planned. This solution, which is still emerging, requires us to support strong constraints from the political and socio-economic point of view and for coastal managers.

Author Contributions: Conceptualization, A.N.L.; methodology, A.N.L. and J.B.; project administration, T.B.; resources, T.B.; supervision, A.N.L.; writing—original draft, A.N.L. and J.B.; writing—review and editing, C.M. All authors have read and agreed to the published version of the manuscript.

Funding: This research received no external funding.

Data Availability Statement: Beach profiles data and LiDAR are available at: http://www.observatoire-cote-aquitaine.fr/ (accessed on 3 April 2022).

Acknowledgments: The authors are grateful to the Observatoire de la Côte Nouvelle-Aquitaine (OCNA) and Brgm for providing data and support. All co-founders of the OCNA project are thanked. We thank the SLGBC of Lacanau for sharing data, in particular bathymetric survey. We thank the anonymous reviewers for their constructive comments, which contribute to improve the manuscript.

Conflicts of Interest: The authors declare no conflict of interest.

References

1. Dean, R.G.; Dalrymple, R.A. *Coastal Processes with Engineering Applications*; Cambridge University Press: Cambridge, UK, 2004.
2. Kamphuis, J.W. *Introduction to Coastal Engineering and Management*; World Scientific: Singapore, 2020; p. 48.
3. Dean, R.G. Coastal Arrnoring: Effects, Principles and Mitigation. In Proceedings of the 20th Coastal Engineering, Taipei, Taiwan, 9–14 November 1986.
4. Weggel, J.R. Seawalls: The need for research, dimensional considerations and a suggested classification. *J. Coast. Res.* **1988**, 29–39. Available online: https://www.jstor.org/stable/25735350 (accessed on 26 February 2022).
5. Pilkey, O.H.; Wright, H.L., III. Seawalls versus beaches. *J. Coast. Res.* **1988**, 41–64. Available online: https://www.jstor.org/stable/25735351 (accessed on 26 February 2022).
6. Griggs, G.B. The interaction of seawalls and beaches: Seven years of monitoring. *Shore Beach* **1994**, *62*, 32–38.
7. Allsop, N.W.H.; McKenna, J.E.; Vicinanza, D.; Whittaker, T.T.J. New design methods for wave impact loadings on vertical breakwaters and seawalls. In Proceedings of the 25th International Conference on Coastal Engineering, Orlando, FL, USA, 2–6 September 1996; pp. 2508–2521.
8. Zheng, J.-H.; Jeng, D.-S.; Mase, H. Sandy beach profile response to sloping seawalls: An experimental study. *J. Coast. Res.* **2007**, *SI 50*, 334–337.
9. Barnett, M.R.; Wang, H. Effects of a Vertical Seawall on Profile Response. In Proceedings of the 21st Coastal Engineering Conference, Costa del Sol-Malaga, Spain, 20–25 June 1988; pp. 1493–1507.
10. Kamphuis, J.W.; Rakha, K.A.; Jui, J. Hydraulic model experiments on seawalls. In Proceedings of the 23rd International Conference on Coastal Engineering, Venice, Italy, 4–9 October 1992; pp. 1272–1284.
11. Smallegan, S.M.; Irish, J.L.; Van Dongeren, A.R.; Den Bieman, J.P. Morphological response of a sandy barrier island with a buried seawall during Hurricane Sandy. *Coast. Eng.* **2016**, *110*, 102–110. [CrossRef]
12. Plant, N.G.; Griggs, G.B. Interactions between nearshore processes and beach morphology near a seawall. *J. Coast. Res.* **1992**, *8*, 183–200.
13. Dean, R.G. Equilibrium beach profiles: Characteristics and applications. *J. Coast. Res.* **1991**, *7*, 53–84.
14. Beuzen, T.; Turner, I.L.; Blenkinsopp, C.E.; Atkinson, A.; Flocard, F.; Baldock, T.E. Physical model study of beach profile evolution by sea level rise in the presence of seawalls. *Coast. Eng.* **2018**, *136*, 172–182. [CrossRef]
15. McCarroll, R.J.; Masselink, G.; Valiente, N.G.; Scott, T.; Wiggins, M.; Kirby, J.A.; Davidson, M. A rules-based shoreface translation and sediment budgeting tool for estimating coastal change: ShoreTrans. *Mar. Geol.* **2021**, *435*, 106466. [CrossRef]
16. Griggs, G.B.; Tait, J.F. Observations on the end-effects of seawalls. *Shore Beach* **1989**, *57*, 25–26.
17. Uda, T. Is the Presence of Seawalls and Concrete Armor Blocks the Cause of Foreshore Erosion? In Proceedings of the 49th Annual Conference 0/1 Ciuil Engineering, Japan Society of Civil Engineers; 1989; pp. 42–43. (In Japanese).
18. Kraus, N.C.; Smith, J.M. Supertank Laboratory Data Collection Project. In Proceedings of the 23rd International Conference on Coastal Engineering, Venice, Italy, 4–9 October 1992.
19. Kraus, N.C.; McDougal, W.G. The effects of seawalls on the beach: Part I, an updated literature review. *J. Coast. Res.* **1996**, *12*, 691–701.
20. McDougal, W.G.; Sturtevant, M.A.; Komar, P.D. Laboratory and Field Investigations of the Impact of Shoreline Stabilization Structures on Adjacent Properties. In Proceedings of the Coastal Sediments'87 American Society of Civil Engineers, 12 May 1987; pp. 961–973. Available online: https://cedb.asce.org/CEDBsearch/record.jsp?dockey=0051611 (accessed on 26 February 2022).
21. Toue, T.; Wang, H. Three dimensional effects of seawall on the adjacent beach. In Proceedings of the 22nd International Conference on Coastal Engineering, Delft, The Netherlands, 2–6 July 1990; pp. 2782–2795.
22. Basco, D.R. Seawall impacts on adjacent beaches: Separating fact from fiction. *J. Coast. Res.* **2006**, *2*, 741–744.
23. Griggs, G.B. The impacts of coastal armoring. *Shore Beach* **2005**, *73*, 13–22.
24. Rakha, K.A.; Kamphuis, J.W. A morphology model for an eroding beach backed by a seawall. *Coast. Eng.* **1997**, *30*, 53–75. [CrossRef]
25. Mossa, J.; Nakashima, L.D. Changes along a seawall and natural beaches: Fourchon, LA. In *Coastal Zone'89, Proceedings of the Sixth Symposium on Coastal and Ocean Management, Charleston, SC, USA, 11–14 July 1989*; ASCE: New York, NY, USA, 1989; Volume 4, pp. 3723–3737.
26. Nelson, D.D. Factors effecting beach morphology changes caused by Hurricane Hugo, northern South Carolina. *J. Coast. Res.* **1991**, 163–179.
27. FitzGerald, D.M.; van Heteren, S.; Montello, T.M. Shoreline processes and damage resulting from the Halloween Eve storm of 1991 along the north and south shores of Massachusetts Bay, USA. *J. Coast. Res.* **1994**, *10*, 113–132.
28. Morton, R.A. Effects of Hurricane Eloise on beach and coastal structures, Florida Panhandle. *Geology* **1976**, *4*, 277–280. [CrossRef]
29. Irish, J.L.; Lynett, P.J.; Weiss, R.; Smallegan, S.M.; Cheng, W. Buried relic seawall mitigates Hurricane Sandy's impacts. *Coast. Eng.* **2013**, *80*, 79–82. [CrossRef]
30. Griggs, G.B.; Tait, J.F.; Moore, L.J.; Scott, K.; Corona, W.; Pembrook, D. *Interaction of Seawalls and Beaches: Eight Years of Field Monitoring, Monterey Bay, California*; U.S. Army Corps of Engineers, Waterways Experiment Station, Contract Rpt. CHL-97-1; 1997; 34p, Available online: https://apps.dtic.mil/sti/citations/ADA323871 (accessed on 26 February 2022).
31. Basco, D.R.; Bellomo, D.A.; Hazelton, J.M.; Jones, B.N. The influence of seawalls on subaerial beach volumes with receding shorelines. *Coast. Eng.* **1997**, *30*, 203–233. [CrossRef]

32. Lafon, V.; Froidefond, J.M.; Lahet, F.; Castaing, P. SPOT shallow water bathymetry of a moderately turbid tidal inlet based on field measurements. *Remote Sens. Environ.* **2002**, *81*, 136–148. [CrossRef]
33. Castelle, B.; Marieu, V.; Bujan, S. Alongshore-variable beach and dune changes on the timescales from days (storms) to decades along the rip-dominated beaches of the Gironde Coast, SW France. *J. Coast. Res.* **2019**, *88*, 157–171. [CrossRef]
34. Castelle, B.; Marieu, V.; Bujan, S.; Splinter, K.D.; Robinet, A.; Sénéchal, N.; Ferreira, S. Impact of the winter 2013–2014 series of severe Western Europe storms on a double-barred sandy coast: Beach and dune erosion and megacusp embayments. *Geomorphology* **2015**, *238*, 135–148. [CrossRef]
35. Castelle, B.; Bujan, S.; Ferreira, S.; Dodet, G. Foredune morphological changes and beach recovery from the extreme 2013/2014 winter at a high-energy sandy coast. *Mar. Geol.* **2017**, *385*, 41–55. [CrossRef]
36. Nicolae Lerma, A.; Ayache, B.; Ulvoas, B.; Paris, F.; Bernon, N.; Bultreau, T.; Mallet, C. Pluriannual beach-dune evolutions at regional scale: Erosion and recovery sequences analysis along the Aquitaine coast based on airborne LiDAR data. *Cont. Shelf Research.* **2019**, *189*, 103974. [CrossRef]
37. Bossard, V.; Lerma, A.N. Geomorphologic characteristics and evolution of managed dunes on the South West Coast of France. *Geomorphology* **2020**, *367*, 107312. [CrossRef]
38. Nicolae Lerma, A.; Castelle, B.; Marieu, V.; Robinet, A.; Bulteau, T.; Bernon, N.; Mallet, C. Decadal beach-dune profile monitoring along a 230-km high-energy sandy coast: Aquitaine, southwest France. *Appl. Geogr.* **2022**, *139*, 102645. [CrossRef]
39. SOGREAH. *Littoral de la Gironde—Evolution Prévisible*; Préfecture de la Gironde, Rapport Réf. SOGREAH 51 1456/JMG, Décembre 1994, Actualisation Juin 1995; p. 70. Available online: https://archimer.ifremer.fr/doc/00370/48071/48172.pdf (accessed on 26 February 2022).
40. BRGM; IFREMER. *Élaboration d'un Outil de Gestion Prévisionnelle de la Côte Aquitaine. Phase 1: Reconnaissance, Évolution historique*; Rapport de synthèse. Rap. BRGM R 39882-IFREMER R.INT.DEL/97.12; 1998; p. 78. Available online: https://archimer.ifremer.fr/doc/00082/19321/ (accessed on 26 February 2022).
41. Bernon, N.; Mallet, C.; Belon, R. *Caractérisation de L'aléa Recul du Trait de Côte sur le Littoral de la Côte Aquitaine Aux Horizons 2025 et 2050: Rapport Final*; BRGM/RP-66277-FR, 99 pp., 48 Ill., 16 tab., 2 ann., 1 CD; 2016; Available online: https://side.developpement-durable.gouv.fr/Default/doc/SYRACUSE/355570/caracterisation-de-l-alea-recul-du-trait-de-cote-sur-le-littoral-de-la-cote-aquitaine-aux-horizons-2 (accessed on 26 February 2022).
42. Castelle, B.; Guillot, B.; Marieu, V.; Chaumillon, E.; Hanquiez, V.; Bujan, S.; Poppeschi, C. Spatial and temporal patterns of shoreline change of a 280-km high-energy disrupted sandy coast from 1950 to 2014: SW France. *Estuar. Coast. Shelf Sci.* **2018**, *200*, 212–223. [CrossRef]
43. Masselink, G.; Castelle, B.; Scott, T.; Dodet, G.; Suanez, S.; Jackson, D.; Floc'h, F. Extreme wave activity during 2013/2014 winter and morphological impacts along the Atlantic coast of Europe. *Geophys. Res. Lett.* **2016**, *43*, 2135–2143. [CrossRef]
44. Nicolae Lerma, A.; Bulteau, T.; Lecacheux, S.; Idier, D. Spatial variability of extreme wave height along the Atlantic and channel French coast. *Ocean. Eng.* **2015**, *97*, 175–185. [CrossRef]
45. Tucker, M.J.; Pitt, E.G. *Waves in ocean Engineering*; Elsevier: Oxford, UK, 2001.
46. Clus-Auby, C. *La Gestion de L'érosion Des Côtes: L'exemple Aquitain*; Presses Univ de Bordeaux: Pessac, France, 2003; p. 40.
47. Biausque, M.; Senechal, N. Seasonal morphological response of an open sandy beach to winter wave conditions: The example of Biscarrosse beach, SW France. *Geomorphology* **2019**, *332*, 157–169. [CrossRef]
48. Komar, P.D. Beach Processes and Sedimentation. 1998, p. 544. Available online: https://agupubs.onlinelibrary.wiley.com/doi/abs/10.1029/98EO00170 (accessed on 26 February 2022).
49. Pilkey, O.H.; Cooper, J.A.G. "Alternative" shoreline erosion control devices: A review. In *Pitfalls of Shoreline Stabilization*; Springer: Dordrecht, The Netherlands, 2012; pp. 187–214.
50. Tait, J.F.; Griggs, G.B. Beach Response to the Presence of a Seawall. *Shore Reach.* **1990**, *58*, 11–28.
51. Balaji, R.; Sathish Kumar, S.; Misra, A. Understanding the effects of seawall construction using a combination of analytical modelling and remote sensing techniques: Case study of Fansa, Gujarat, India. *Int. J. Ocean. Clim. Syst.* **2017**, *8*, 153–160. [CrossRef]
52. Kraus, N.C. The effects of seawalls on the beach: An extended literature review. *J. Coast. Res.* **1988**, 1–28. Available online: https://www.jstor.org/stable/25735349 (accessed on 26 February 2022).
53. Griggs, G.B.; Tait, J.F.; Scott, K.; Plant, N. The interaction of seawalls and beaches: Four years of field monitoring, Monterey Bay, California. In *Coastal Sediments*; ASCE: New York, NY, USA, 1991; pp. 1871–1885.
54. Paskoff, R. Aspects de la recherche en géomorphologie littorale/Current research in coastal geomorphology. *Géomorphologie Relief Processus Environ.* **2001**, *7*, 3–4.
55. Miles, J.R.; Russell, P.E.; Huntley, D.A. Field measurements of sediment dynamics in front of a seawall. *J. Coast. Res.* **2001**, *17*, 195–206.
56. Morton, R.-A. Interactions of storms, Seawalls, and Beaches of the Texas Coast. *J. Coast. Res.* **1988**, 113–134. Available online: https://www.jstor.org/stable/25735355 (accessed on 26 February 2022).
57. Samat, O.; Sabatier, F.; Lambert, A. Bathymetric impacts of a seawall on a micro-tidal beach, Gulf of Lions, France. *Méditerranée Rev. Géographique Des Pays Méditerranéens/J. Mediterr. Geogr.* **2007**, *108*, 119–124. [CrossRef]

58. Ruiz de Alegria-Arzaburu, A.; García-Nava, H.; Gil-Silva, E.; Desplán-Salinas, G. A morphodynamic comparison of walled and non-walled beach sections, Ensenada beach. Mexico. In *World Scientific, The Proceedings of the Coastal Sediments*; Available online: https://www.worldscientific.com/doi/abs/10.1142/9789814689977_0018 (accessed on 26 February 2022).
59. Mendes, D.; Pais-Barbosa, J.; Baptista, P.; Silva, P.A.; Bernardes, C.; Pinto, C. Beach Response to a Shoreface Nourishment (Aveiro, Portugal). *J. Mar. Sci. Eng.* **2015**, *9*, 1112. [CrossRef]
60. Kriebel, D.L. Beach recovery following hurricane Elena. In *Coastal Sediments*; ASCE: New York, NY, USA, 1987; pp. 990–1005.
61. Ruggiero, P.; McDougal, W.G. An analytic model for the prediction of wave setup, longshore currents and sediment transport on beaches with seawalls. *Coast. Eng.* **2001**, *43*, 161–182. [CrossRef]
62. Birkemeier, W.A.; Bichner, E.W.; Scarborough, B.L.; McConathy, M.A.; Eiser, W.C. Nearshore profile response caused by Hurricane Hugo. *J. Coast. Res.* **1991**, 113–127. Available online: https://www.jstor.org/stable/25735411 (accessed on 26 February 2022).
63. Hanson and Kraus Seawall Constraint in the Shoreline Numerical Model. Journal o] Waterway, Port. *Coast. Ocean. Eng.* **1985**, *111161*, 1079–1083.
64. Dean, R.G.; Yoo, C.H. Beach nourishment in presence of seawall. *J. Waterw. Port Coast. Ocean. Eng.* **1994**, *120*, 302–316. [CrossRef]
65. Idier, D.; Castelle, B.; Charles, E.; Mallet, C. Longshore sediment flux hindcast: Spatio-temporal variability along the SW Atlantic coast of France. *J. Coast. Res.* **2013**, *165*, 1785–1790. [CrossRef]
66. Hallermeier, R.J. A profile zonation for seasonal sand beaches from wave climate. *Coast. Eng.* **1981**, *4*, 253–277. [CrossRef]
67. Birkemeier, W.A. Field data on seaward limit of profile change. *J. Waterw. Port Coast. Ocean. Eng.* **1985**, *111*, 598–602. [CrossRef]
68. Hearon, G.E.; McDougal, W.G.; Komar, P.D. Long-term beach response to shore stabilization structures on the Oregon coast. In Proceedings of the 25th International Conference on Coastal Engineering, Orlando, FL, USA, 2–6 September 1996; pp. 2718–2731.
69. Ruggiero, P. Impacts of shoreline armoring on sediment dynamics. In *Puget Sound Shorelines and the Impacts of Armoring—Proceedings of a State of the Science Workshop, May 2009: U.S. Geological Survey Scientific Investigations Report 2010–5254*; Shipman, H., Dethier, M.N., Gelfenbaum, G., Fresh, K.L., Dinicola, R.S., Eds.; 2010; pp. 179–186. Available online: https://www.researchgate.net/profile/Peter-Ruggiero/publication/303152740_Impacts_of_Shoreline_Armoring_on_Sediment_Dynamics/links/54cf9c9a0cf29ca810ff4d53/Impacts-of-Shoreline-Armoring-on-Sediment-Dynamics.pdf (accessed on 26 February 2022).
70. LCHF. *Etude en Nature de la Côte Aquitaine (Entre la Pointe de Grave et L'embouchure de L'adour)*; Rapport pour la Mission Interministérielle pour pour l'Aménagement de la Côte Aquitaine; Laboratoire Central Hydraulique de France: Paris, France, 1979; pp. 13–36. (In French)